ACS OMEGA

http://pubs.acs.org/journal/acsodf

Article

Experimental Measurement and Equilibrium Modeling of Adsorption of Asphaltenes from Various Origins onto the Magnetite Surface under Static and Dynamic Conditions

Mohammad-Reza Mohammadi,* Sajjad Ansari, Hamid Bahmaninia, Mehdi Ostadhassan,* Saeid Norouzi-Apourvari, Abdolhossein Hemmati-Sarapardeh,* Mahin Schaffie, and Mohammad Ranjbar

Cite This: *ACS Omega* 2021, 6, 24256−24268

Read Online

ACCESS | Metrics & More | Article Recommendations | Supporting Information

ABSTRACT: Wettability alterations, permeability reduction of reservoir rocks, and oil production decline may occur as a consequence of asphaltene adsorption and deposition on the surfaces of oil reservoir rocks. Magnetite and other iron minerals are abundant in the rock composition of sandstone reservoirs and cause problems by precipitation and adsorption of polar components of crude oil. The main purpose of this study was to investigate the adsorption of six asphaltene samples of various origins onto the magnetite surface. Characterization of magnetite was performed by Brunauer−Emmett−Teller (BET), Fourier transform infrared spectroscopy (FTIR), and X-ray fluorescence (XRF). Also, FTIR, dynamic light scattering (DLS), and elemental analysis were performed to characterize asphaltenes. Static and dynamic adsorption experiments were carried out to investigate the effects of the water phase, adsorbent size, flow rate, and asphaltene compositions on asphaltene uptake by the magnetite. The results showed that an increase in the nitrogen content and aromatic nature of asphaltenes increased their adsorption on magnetite. The addition of water to the adsorption tests significantly reduced the adsorption amount of asphaltenes on the magnetite. A considerable decrease in asphaltene adsorption was observed with an increase in the flow rate in dynamic tests. This shows that higher flow rates reduce the interaction between adsorbed asphaltenes and asphaltene aggregates in the solution, which reduces the uptake of more asphaltenes. Moreover, adsorbed asphaltene components with a weaker bond are detached from the magnetite surface, which can be attributed to the physisorption of asphaltenes. Eventually, four well-known adsorption isotherm models, namely, Langmuir, Dubinin−Radushkevich, Temkin, and Freundlich were utilized to find the mechanisms of asphaltene adsorption onto the magnetite surface. The Freundlich model seems to provide better estimates for the adsorption of asphaltenes on the magnetite surface. The findings of this study render insights into the better management of oil production in formations with iron-containing rocks.

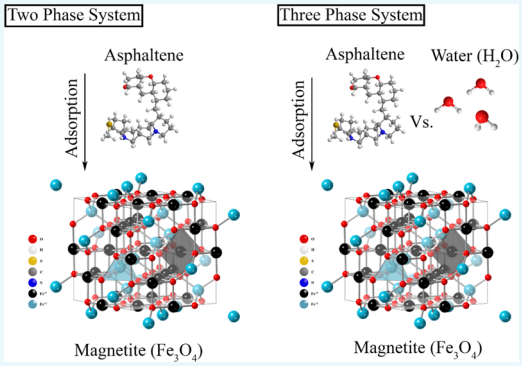

1. INTRODUCTION

The heaviest and most polar fraction of crude oil that is soluble in aromatic fluids and insoluble in alkanes is defined as asphaltene.[1] As the pressure, temperature, and chemical composition of the crude oil change due to reservoir depletion and addition of liquids or gas for enhanced oil recovery (EOR) purposes, asphaltene precipitation may occur.[2] Because of its different functional groups and high polarity, asphaltene can cause many problems such as wettability alterations, plugging of rock pores, and permeability reduction of reservoir rocks in the oil reservoir. The adsorption and deposition of asphaltene on the surface of reservoir rocks can eventually lead to oil production decline.[1,3,4] Coating of the rock surface by polar molecules such as asphaltene or even resin is often cited as the main reason for the wettability alteration of reservoir rocks.[5] Hence, the study of adsorption of asphaltenes onto the surface of reservoir rocks and solid−fluid interaction with rock minerals is very important to gain insight into the better management of oil production in formations.[6,7] However, the lack of definite information about asphaltene interactions with different rock mineralogy and its behavior in different fluid environments due to the complexity of the asphaltene molecule has made this topic an attractive area for research.

It has been well-established that the aggregation behavior in toluene−normal alkane mixtures, molecular weight, heteroa-

Received: August 6, 2021
Published: September 10, 2021

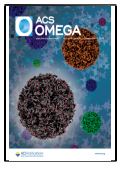

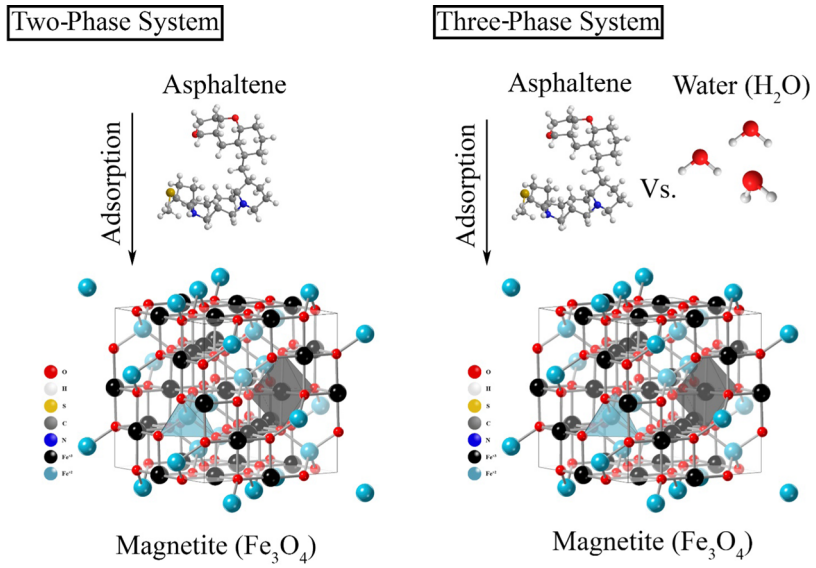

Figure 1. Molecular sketch of the problem under consideration in this work.

toms content, alkyl side chain length, and amount of aromatic compounds for the asphaltenes extracted from crude oils of diverse origins are different.[8,9] The precipitation and deposition of asphaltenes are highly dependent on their structure and compositions. The nature of asphaltenes affects the stability of crude oils, and their polar and aromatic groups along with heteroatomic functional groups contribute to their adsorption on the surfaces of charged particles of reservoir rock minerals.[10−13]

Magnetite (Fe_3O_4) has high solubility because of the formation of Fe^{2+} complexes with chloride,[14] and it has special surface chemistry and surface charge retention properties even at high temperatures, which makes it a strong adsorbent.[15,16] The solid particles of corrosion products (e.g., Fe_3O_4 from pipelines) present in produced water may adsorb surface-active components (e.g., asphaltenes) upon contact with oil and have destructive effects when they are re-injected into the reservoir.[17] Normally, more iron minerals exist in sandstone formations compared to the carbonate ones. Iron-containing minerals such as magnetite, hematite, ankerite, and pyrite, due to precipitation of ferrous and ferric ions, provide sites for the adsorption of asphaltene polar molecules. Subsurface processes such as migration of cations and anions in the porous media, mineral dissolution and kinetics, and transport of colloidal particles are influenced by a fundamental phenomenon of the adsorption of ions to rock surfaces.[14] Well operations such as acidizing, treatment after drilling operation, and low salinity water flooding cause pH alteration in the reservoir, which change the surfaces of the rock. This phenomenon leads to fluid−rock interactions and mineral particle precipitation. Therefore, it causes a change in surface chemistry and promotes the uptake of asphaltenes by the rock surface.[18,19] Thus, the existence of iron-containing minerals in reservoir rocks is a concern, especially when these minerals are in contact with crude oil.

Researchers have always considered the adsorption of asphaltene onto various surfaces as an important phenomenon.[1,20−29] González and Middea[30] showed that the adsorption of asphaltene on calcite was higher than that of resin.[30] Marczewski and Szymula[23] demonstrated that the concentration of asphaltene solutions dictates the asphaltene adsorption model.[23] Dudášová et al.[31] by examining the adsorption of five asphaltenes onto several inorganic particles showed that a direct correlation exists between the adsorbed amount on the particles and the amount of nitrogen in asphaltenes.[31] Gonzalez and Taylor[32] revealed that the existence of preadsorbed water decreased the amount of asphaltene uptake by the adsorbent.[32] Khormali et al.[33] experimentally indicated that increasing the initial concentration of asphaltene increased the adsorption onto sandstone and carbonate rocks and the presence of asphaltene inhibitors reduced the amount of asphaltene uptake.[33] Monjezi et al.[34] by performing dynamic adsorption tests showed that the presence of a brine film forms a mechanical barrier between the surface of the adsorbent and asphaltenes and leads to a significant decrease in asphaltene uptake.[34] Ahooei et al.[11] performed an experimental investigation and modeling of asphaltene deposition on metal surfaces and showed that the structure and composition of asphaltenes highly affected their deposition amount.[11] Mohammed et al.[18] studied the effect of iron minerals (pyrite, hematite, and magnetite) in increasing wettability alterations of the reservoir rock. Their results indicated that iron minerals promoted asphaltene adsorption and mineral scale formation, which induced alterations in the surface charge. Also, magnetite was introduced as the most critical iron mineral and posed serious concerns.[18] Moreover, it has been shown that magnetite nanoparticles have applicability in EOR operations by providing adsorption sites for oil colloidal components along with other properties such as magneto-responsive properties and reduction in interfacial tension of water and oil.[35−40] Kazemzadeh et al.[41] experimentally showed that Fe_3O_4 nanoparticles considerably decreased the asphaltene flocculation in the porous media by adsorption of asphaltene particles, which subsequently reduced the formation damages.[41] Nassar et al.[42] experimentally demonstrated that a decrease in the molecular weight of asphaltenes increased the extent of their adsorption onto Fe_3O_4 nanoparticles. Also, the high affinity of Fe_3O_4 nanoparticles for the adsorption of asphaltenes significantly decreases the average activation energy and oxidation temperature, which serve as a unique catalyst/adsorbent for the upgrading of heavy oil.[42] Tazikeh et al.[40] demonstrated that asphaltenes are adsorbed more on polythiophene-coated Fe_3O_4 nanoparticles in heavy oil, compared to light oil. Also, fewer or/and smaller agglomerates of asphaltenes

https://doi.org/10.1021/acsomega.1c04224
ACS Omega 2021, 6, 24256−24268

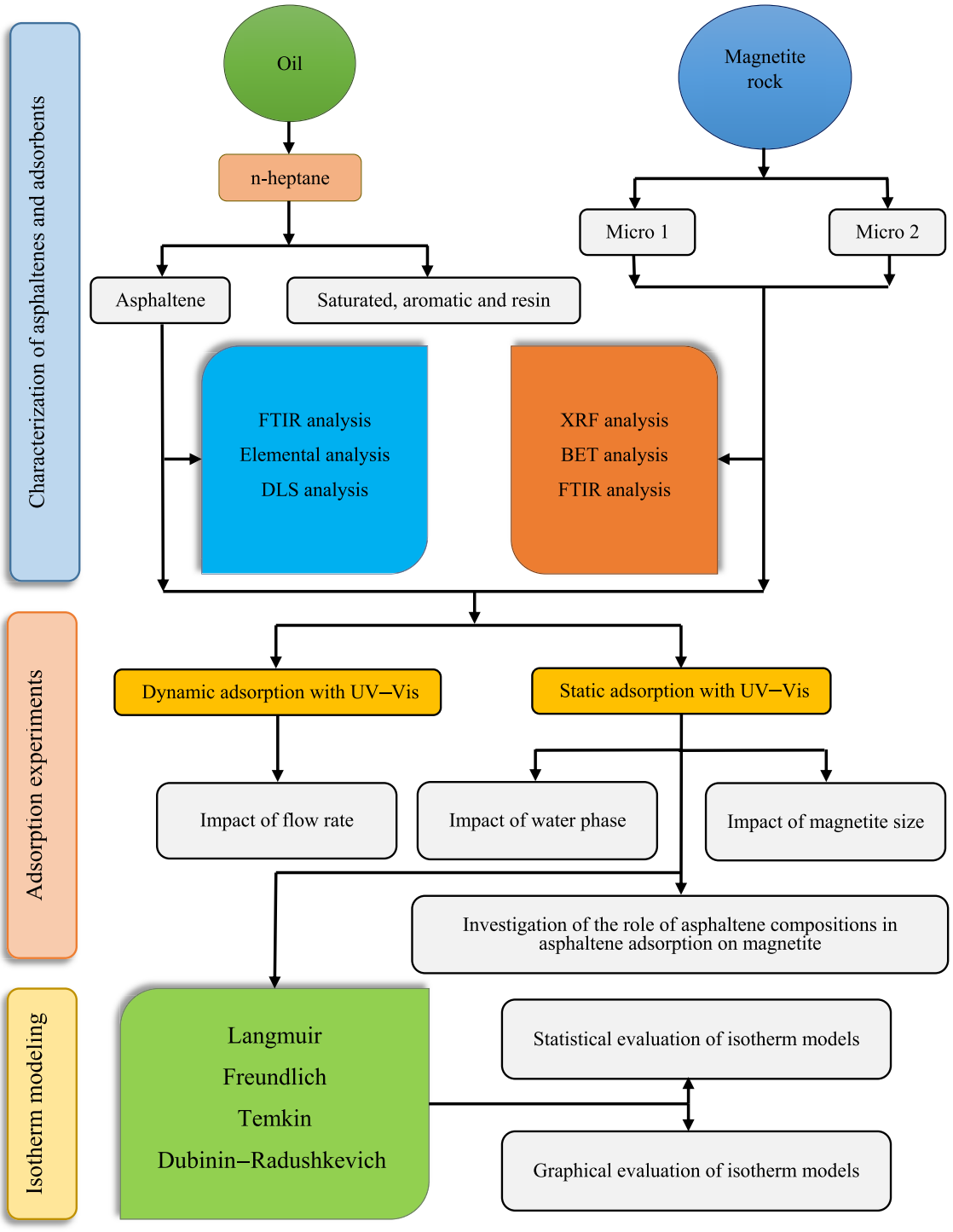

Figure 2. Schematic of the research steps in this work.

precipitate in the presence of nanoparticles. In another study, Tazikeh et al.[43] showed that aromatic rings and functional groups in the asphaltene structure are involved in the adsorption of asphaltenes onto polythiophene-coated Fe_3O_4 nanoparticles. Mousavi et al.[44] showed that asphaltene has more impact on the wettability alteration of dolomite and calcite rocks toward oil-wet state compared to resin.

According to the aforementioned research studies on asphaltene adsorption onto different surfaces, it can be stated that iron oxide particles, especially magnetite, have a serious role in asphaltene adsorption and their presence in the oil reservoir in any form can be troublesome. Also, the adsorption behavior of various asphaltenes can be different due to their different structures and composition. However, most studies on asphaltene adsorption on iron-containing minerals are likely to yield case-specific results due to the limited number of asphaltenes used. Also, the impacts of asphaltene composition, flow rate, and water phase on asphaltene adsorption onto magnetite have been less considered. We have recently conducted a research study on the role of different asphaltenes in their adsorption on quartz as the main mineral of sandstone reservoirs,[45] and in this study, we examined the adsorption

https://doi.org/10.1021/acsomega.1c04224
ACS Omega 2021, 6, 24256−24268

behavior of different asphaltenes onto magnetite to get an in-depth look at the better management of oil production in iron-containing rocks in sandstone formations. Figure 1 depicts the molecular sketch of the problem under consideration in this work.

In the current work, the adsorption of six asphaltene samples of various origins onto the magnetite surface is investigated. First, the characterization of magnetite is performed by Brunauer–Emmett–Teller (BET), Fourier transform infrared spectroscopy (FTIR), and X-ray fluorescence (XRF). Also, FTIR, dynamic light scattering (DLS), and elemental analysis are used to characterize asphaltenes. Then, static and dynamic adsorption experiments are carried out to investigate the effects of the water phase, flow rate, and asphaltene compositions on asphaltene uptake by the magnetite. Eventually, four well-known adsorption isotherm models, namely, Langmuir, Dubinin–Radushkevich, Temkin, and Freundlich are utilized to provide information on the mechanism of asphaltene adsorption onto the magnetite surface.

2. EXPERIMENTS AND METHODS

The schematic of the research steps in this work is presented in Figure 2. The problem under study is investigated by performing three steps of characterization of asphaltenes and magnetite adsorbents, asphaltene uptake experiments, and isotherm modeling.

2.1. Materials. Magnetite is an iron oxide mineral that is used as the adsorbent in this work, with XRF results represented in Table 1. Two sizes of magnetite adsorbents were utilized for the adsorption tests. Their specific surface areas (BET method) and specifications are reported in Table 2. As reported in Table 2, the pores of both magnetite adsorbents are in the range of 2–50 nm and can be categorized into mesopore classes.[46] It is better to mention that PW1410 (PHILIPS, Netherland) and BELSORP mini II (Microtrac Bel Corp, Japan) were used to conduct XRF and BET analyses, respectively. FTIR of magnetite adsorbents was also recorded using TENSOR 27 (Brucker, Germany). Figure 3 shows the FTIR spectrum of the magnetite adsorbent. Fe–O stretching vibration is observed at a wavelength of 560 cm^{-1}, which is the approximate characteristic peak of iron oxide.[47] Also, peaks of 1629, 3396, and 3462 cm^{-1}, which are attributed to the presence of hydroxyl functional groups on magnetite particles, can be seen in the figure. Due to the presence of hydroxyl groups on the surface of iron oxides, it can be stated that the structure of adsorbent particles is hydrophilic.[48]

Table 1. Results of XRF Analysis of Magnetite[29]

compound	contents (wt %)
SiO_2	2.82
Al_2O_3	0.29
total Fe	54.31
CaO	2.35
K_2O	<0.01
BaO	<0.01
MgO	9.47
MnO	0.05
Na_2O	0.06
S	1.91
P	0.24
TiO_2	0.01
Cr_2O_3	<0.01
Zn	<0.01
Pb	<0.01
Cu	<0.01
loss on ignition	6.89

Table 2. Specification of Magnetite Adsorbents[29]

adsorbent	pore volume (cm^3/g)	specific surface area (BET) (m^2/g)	mean pore diameter (nm)	particle size (μm)
micro-magnetite 1	0.0021	0.3127	26.73	80–400
micro-magnetite 2	0.0097	1.97	19.67	30–70

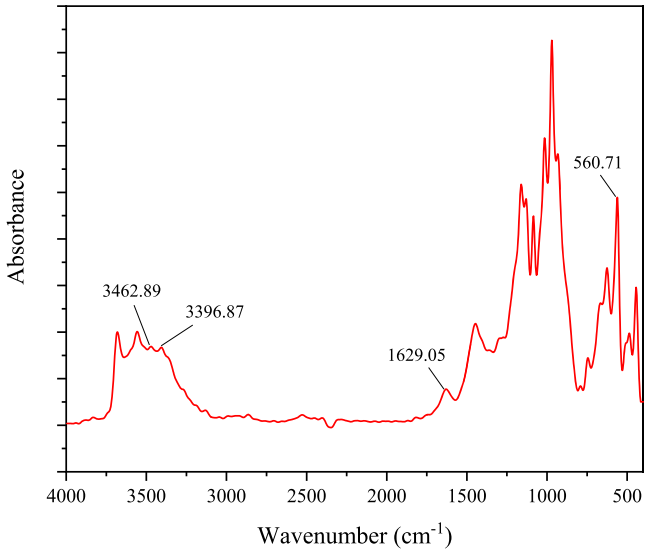

Figure 3. FTIR spectrum of the magnetite adsorbent.

In this study, 3-phase adsorption tests were conducted utilizing Persian Gulf water having a pH of 7.9. Ions of this water include Cl^-, SO_4^{2-}, HCO_3^{2-}, K^+, Na^+, Ca^{2+}, and Mg^{2+} with total dissolved solids of about 41 g/L.[49]

2.2. Methods. *2.2.1. Characterization of Asphaltene Samples.* The standard method of the ASTM standard (D2007-80)[50] was utilized to extract asphaltene samples from six crude oils of various Iranian oil fields. FTIR analysis (Brucker, TENSOR 27, Germany), elemental analysis (Elementar, Vario MACRO, Germany), and DLS analysis (Malvern, ZEN3600, England) were used to determine the functional groups and structures, the constituent elements, and the particle size distribution of asphaltenes, respectively. It is worth noting that several analyses of asphaltenes utilized in this paper are taken from our previous adsorption studies,[29,45] which are cited in the relevant figures and tables.

2.2.2. Two-Phase Static Adsorption Experiments. The static tests of asphaltene adsorption were performed by adding 1 g of magnetite adsorbents to 10 mL solutions of asphaltene/toluene with several concentrations (0, 100, 200, 500, 1000 ppm). A shaker-incubator (Stuart SI 50, England) was used for mixing the mixture of adsorbents and asphaltene solutions for 18 h at a certain temperature of 298 K and atmospheric pressure of 101.325 kPa with 250 rpm speed. It is worth noting that the initial adsorption experiments showed that the adsorption of asphaltenes on the magnetite reached equilibrium within about

https://doi.org/10.1021/acsomega.1c04224
ACS Omega 2021, 6, 24256–24268

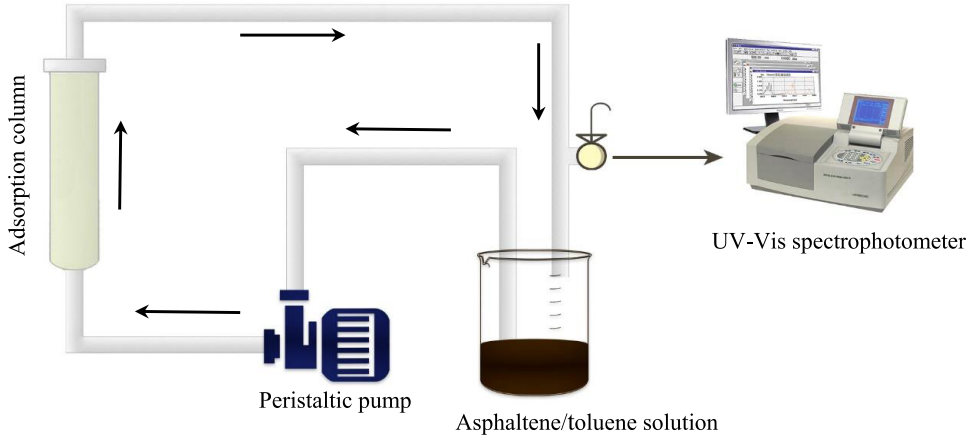

Figure 4. Schematic image of dynamic adsorption experiments.

2 h (Figure S1), but to ensure reaching equilibrium, the contact time of 18 h was considered sufficient for the equilibrium time in static experiments. The extent of asphaltenes adsorbed on magnetite particles was then specified using a UV−vis spectrophotometer at a certain wavelength of λ = 410 nm, which provides adequate sensitivity to specific asphaltene concentrations, and it is within the device absorbance threshold without exceeding the device detection limit.[24,35] Eventually, the extent of adsorbed asphaltenes on magnetite surface was calculated applying the following equation

$$q_e = \frac{V(C_0 - C_e)}{mA} \quad (1)$$

where q_e, V, C_e, C_0, A, and m denote the extent of asphaltene adsorption (mg asphaltenes/m^2 magnetite particles), the solution volume (L), the equilibrium concentration after asphaltene uptake (mg/L), the initial asphaltene concentration (mg/L), the specific surface area of magnetite particles (m^2), and the adsorbent mass (g), respectively.

2.2.3. Three-Phase Static Adsorption Experiments. Unlike other works that initially exposed the mineral to water and then performed the asphaltene adsorption tests, here, magnetite adsorbents were added to a system including asphaltene/toluene solution and water in a ratio of 1:1 to consider the competitive performance of asphaltenes and water in the adsorption process. In this case, the mass of asphaltenes in the organic solution in the 2- and 3-phase systems was the same, and therefore, the effect of the water phase on asphaltene uptake by the magnetite was investigated. It is worth noting that the mixtures of water and asphaltene/toluene solution are stirred before the adsorbent is added and after it is added during continuous testing using the shaker-incubator.

2.2.4. Dynamic Adsorption Experiments. The dynamic adsorption experiments were conducted using a 6 cm height fixed-bed poly(ethylene terephthalate) column with an inner diameter of 2 cm. Figure 4 schematically presents the equipment utilized for the dynamic adsorption experiments. Here, 100 ppm concentration asphaltene/toluene solution was injected into the magnetite-filled column with inlet flow rates of 5, 10, and 15 mL/min. The fluid flow direction was upward to eliminate channeling due to gravity. In this series of dynamic adsorption experiments, micro-magnetite 1 was used as the adsorbent. Again, the adsorbents to solution ratio were selected as 1 g:10 mL. Finally, the adsorption of asphaltenes at certain times (up to 60 min) was calculated using the solution of the column outlet.

2.3. Adsorption Isotherm Models. Four well-known adsorption isotherm models, namely, Langmuir, Dubinin−Radushkevich, Temkin, and Freundlich were utilized to model the adsorption data and provide information on the mechanism of asphaltene adsorption on magnetite. The subsequent equations present the nonlinear form of these isotherm models

Temkin:

$$q_e = \frac{RT}{b} \ln k_T C_e \quad (2)$$

Langmuir:

$$q_e = \frac{Q_m k_L C_e}{1 + k_L C_e} \quad (3)$$

Dubinin−Radushkevich:

$$q_e = (q_s)\exp(-k_{ads}\varepsilon^2) \quad (4)$$

Freundlich:

$$q_e = k_F C_e^{1/n} \quad (5)$$

More information about the above-mentioned isotherm models and their parameters can be obtained in the literature.[51−53]

3. RESULTS AND DISCUSSION

3.1. Characterization of Asphaltene Samples. First, the outcomes of elemental analysis of six asphaltene samples utilized in this work are presented in Table 3. Literature survey demonstrates that H/C molar ratios of six asphaltene samples are similar to other asphaltenes.[35,54] Basically, an asphaltene sample with a lower H/C ratio has a higher aromatic nature.[42,55]

Table 3. Results of Elemental Analysis of Six Asphaltene Samples

	C (%)	H (%)	N (%)	S (%)	O (%)	N + S + O (%)	H/C molar ratio
As-1[45]	80.62	8.64	1.26	5	4.48	10.74	1.276
As-2[29]	82.58	8.35	1.47	3.07	4.53	9.07	1.204
As-3	83.97	9.03	0.94	1.84	4.22	7	1.281
As-4[29]	81.56	8.80	1.13	2.05	6.46	9.64	1.285
As-5[45]	82.35	9.19	0.82	2.66	4.98	8.46	1.329
As-6[45]	81.86	8.79	0.97	3.02	5.36	9.35	1.279

https://doi.org/10.1021/acsomega.1c04224
ACS Omega 2021, 6, 24256−24268

Also, the higher the NSO content for an asphaltene, the higher is its polarity.[45,56] On examining Table 3, it can be stated that asphaltene 2 and 1 samples have the highest and asphaltene 5 has the lowest aromatic nature among the six asphaltene samples. Also, asphaltene 1 has the highest and asphaltene 3 has the lowest polarity among all of the asphaltenes.

In the next step of asphaltene characterization, FTIR spectra of asphaltenes are depicted in Figure 5. Asymmetrical stretching

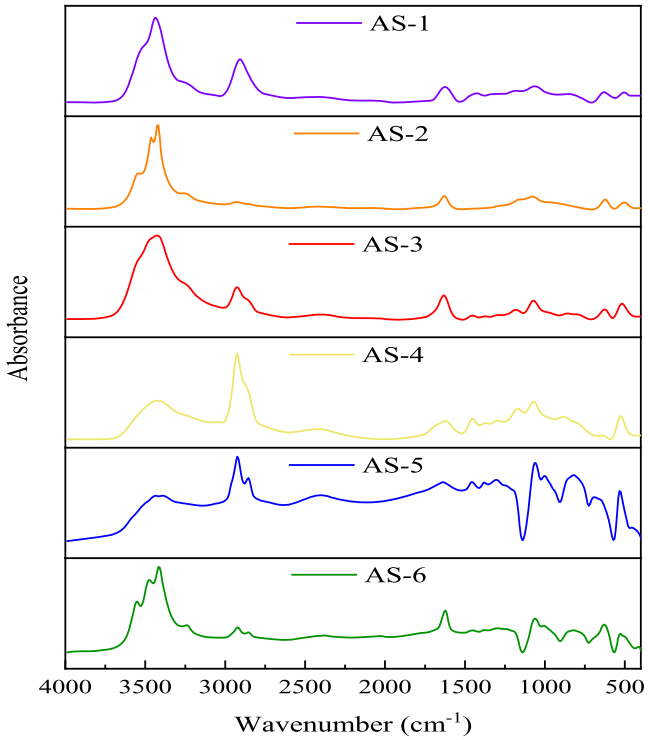

Figure 5. FTIR spectra of all of the asphaltenes.[29,45] Reprinted in part with permission from the authors of another article.[45] Copyright [2021] [Elsevier].

of the C−H bond in CH_2 seen at 2923 cm^{-1} in all of the spectra of asphaltenes was used to perform the normalization process. Moreover, Table S1 represents the major identified peaks and corresponding functional groups for the asphaltene samples.

Several indexes are defined based on the area under the peaks in the FTIR spectra to provide a better insight into asphaltene adsorption behavior with recognition of the structural properties of asphaltenes. Aliphatic, aromatic, and sulphoxide indexes were defined based on the next equations, which refer to all aliphatic compounds, all aromatic compounds, and the frequency of S═O bonds in asphaltenes, respectively.[57,58]

Aliphatic index:

$$\frac{A_{1460} + A_{1376}}{\sum A} \quad (6)$$

Aromatic index:

$$\frac{A_{1600}}{A_{814} + A_{743} + A_{724}} \quad (7)$$

Sulphoxide index:

$$\frac{A_{1030}}{\sum A} \quad (8)$$

$$\sum A = A_{724} + A_{743} + A_{814} + A_{864} + A_{1030} + A_{1376} + A_{1460} + A_{1600} + A_{1700} + A_{2862} + A_{2923} + A_{2953} \quad (9)$$

where A and subscript numbers show the peak area in the spectra and the wavenumber related to the peak, respectively. The values of the above-mentioned indexes for all asphaltene samples were calculated and are reported in Table 4. According to Table 4, asphaltene 2 and 1 samples again have the highest values of the aromatic index, asphaltene 5 has the lowest aromatic index, and the trend of aromatic indexes is consistent with the outcomes of Table 3 (H/C molar ratios of elemental analysis). The results suggest that the asphaltene 2 molecule has more aromatic compounds versus asphaltene 1. The highest and lowest aliphatic index values belong to asphaltene 4 and asphaltene 2, respectively. Also, the frequency of S═O bonds in asphaltene 5 is more and in asphaltene 1 is less than the rest.

Table 4. Structural Parameters of Asphaltenes According to FTIR Analysis

	aliphatic index	aromatic index	sulphoxide index
As-1[45]	0.047	1.315	0.066
As-2[29]	0.010	1.349	0.118
As-3	0.048	0.362	0.128
As-4[29]	0.093	0.307	0.129
As-5[45]	0.039	0.207	0.187
As-6[45]	0.013	0.388	0.111

Figure 6 shows the particle size distribution of all of the asphaltenes utilizing DLS analysis. It is worth noting that 200 ppm solution of asphaltene/toluene for all samples was used to perform DLS analysis at a temperature of 298 K. The mean particle diameters of the asphaltene samples 1−6 are calculated as 46 ± 11, 96 ± 25, 161 ± 44, 265 ± 62, 380 ± 92, and 55 ± 10 nm, respectively. Accordingly, asphaltene 5 has the largest, and asphaltene 1 has the smallest particle size compared to other asphaltenes. We have found a relationship between the sulphoxide index of FTIR analysis and the mean particle size of asphaltenes, so that the higher the asphaltene's sulphoxide index, the larger the mean particle size. Sulphoxide is a highly polar group, such that the higher its frequency in the sample, the

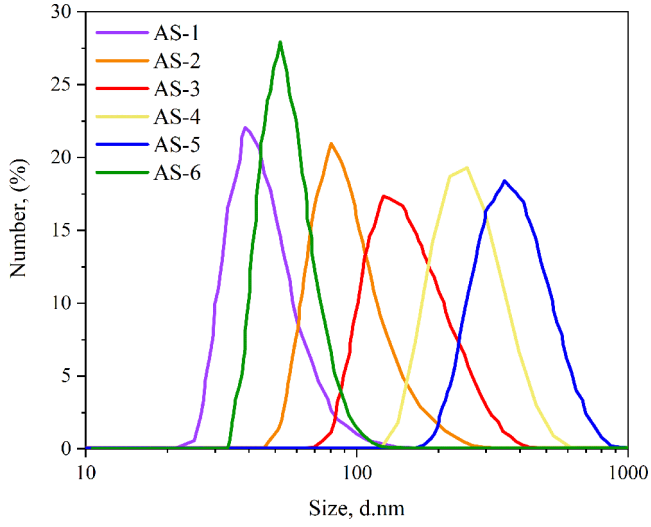

Figure 6. Particle size distribution of all of the asphaltenes.

https://doi.org/10.1021/acsomega.1c04224
ACS Omega 2021, 6, 24256−24268

lower the solubility of asphaltene in toluene[59] and the larger the particle size of asphaltene in the DLS analysis.

3.2. Adsorption Isotherms in Static Experiments. Based on Figure 7, the asphaltene uptake by magnetite adsorbents is highest in the As-2 sample and after that As-1, As-4, As-6, As-3, and As-5 have the highest adsorption, successively. Examining Figure 7a,b, it can be stated that asphaltene uptake (in the context of mg/m^2) onto micro-magnetite 1 is higher than that on micro-magnetite 2. However, our examinations show that due to a higher specific surface area of micro-magnetite 2 than micro-magnetite 1, under similar conditions (mg asphaltene/g adsorbent), the extent of asphaltene uptake by micro-magnetite 2 is higher than that by micro-magnetite 1. As the physical features of adsorbents such as surface area, pore distribution, and inner pore volume are well-known properties that can increase the adsorption capacity,[1,26] the higher asphaltene uptake by micro-magnetite 2 was somewhat anticipated here. It is noteworthy that the As-2 and As-4 isotherm curves have been selected from our previous paper[29] for in-depth comparative analysis.

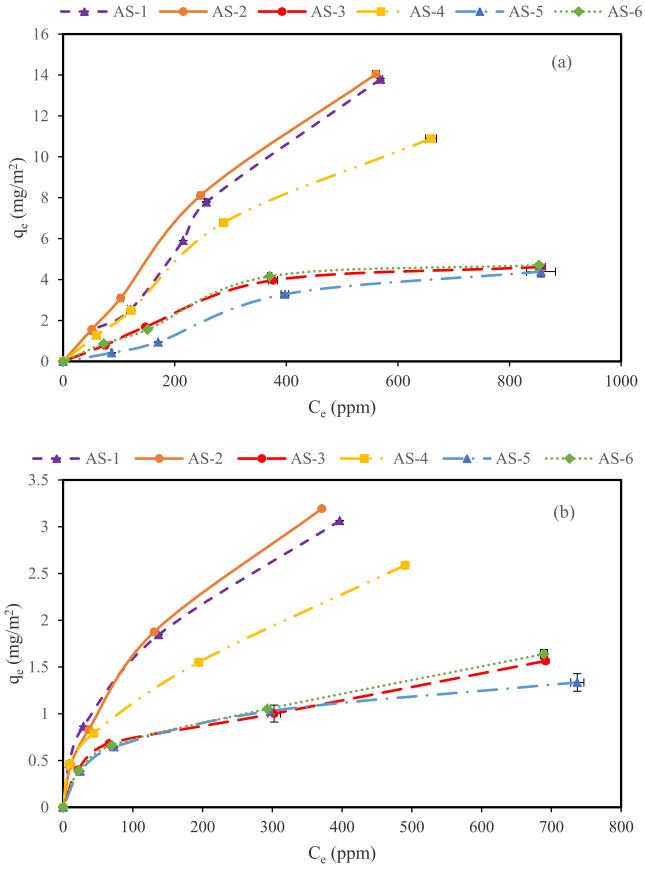

Figure 7. Adsorption isotherms of asphaltene samples onto (a) micro-magnetite 1 and (b) micro-magnetite 2.

3.3. Adsorption of Asphaltenes in Dynamic Experiments. Figure 8 shows the influence of flow rate on the adsorption of the As-1 sample on the adsorbent surface of micro-magnetite 1. Since new feed is not injected into the adsorption column and the output solution from the adsorption column enters the same container as the feed source entering the system, the impact of increasing the energy input to the adsorption system can be investigated in this case. The first point is the equilibrium time of asphaltene uptake, which is extremely fast,

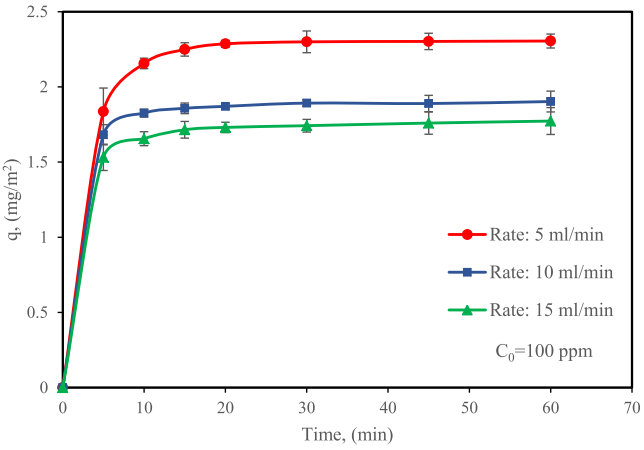

Figure 8. Influence of flow rate on the extent of As-1 adsorption onto micro-magnetite 1.

and in about 15 min, the adsorption reaches equilibrium. The adsorption extent of As-1 decreased from 2.31 to 1.77 mg/m^2 by increasing the flow rate from 5 to 15 mL/min. Basically, adsorbed asphaltene particles tended to interact with smaller aggregates in the solution, which, due to the large radial diffusivity of the particles, have a high tendency to deposit on the adsorbent surface.[60] This significant reduction of about 25% in asphaltene uptake with a threefold increase in flow rate indicates that the higher flow rate reduces the interaction among the adsorbed asphaltene particles and smaller aggregates in the solution that reduces the uptake of more asphaltenes. Also, adsorbed asphaltene components with a weaker bond are released from the magnetite surfaces, which can be attributed to the physisorption of asphaltenes,[29,45] because, unlike chemisorption, physisorption is weak and reversible. It is noteworthy that performing dynamic experiments with asphaltene samples of 2−6 had similar results, such that about 10−25% of the uptake of asphaltene by magnetite particles decreased by increasing 2 and 3 times the flow rate, as shown in Figure S2.

3.4. Adsorption of Asphaltenes in the Presence of Water. Three phases of reservoir rock, crude oil, and water normally exist in a real oil reservoir. The water that exists in the formation can have a significant impact on the adsorption of asphaltene depending on the rock's wettability. Figure 9 compares the asphaltene uptake by magnetite adsorbents in two- (magnetite + asphaltene/toluene solution) and three-phase (water + magnetite + asphaltene/toluene solution) systems. Based on the results, the asphaltene adsorption for all of the samples and both magnetite adsorbents in the 3-phase state and the existence of the water phase is considerably reduced; the asphaltenes adsorption in the 2-phase state was at least 1.2 and at most 3 times that of the three-phase state. Actually, it can be stated that not only water and asphaltene compete for surface adsorption but also the adsorbed water may be considered as a barrier to asphaltene adsorption. The presence of water can highly alter the interactions of hydrogen bonds that are essential for the interactions of asphaltenes/asphaltenes and asphaltenes/adsorbents. However, water cannot totally hinder the uptake of asphaltenes.[1] As mentioned earlier, due to the presence of hydroxyl groups on the surface of magnetite (Figure 3), it can be stated that the structure of the adsorbent particles is hydrophilic and one of the important reasons for the decrease in asphaltenes uptake in the 3-phase adsorption experiments was the hydrophilicity of magnetite

https://doi.org/10.1021/acsomega.1c04224
ACS Omega 2021, 6, 24256−24268

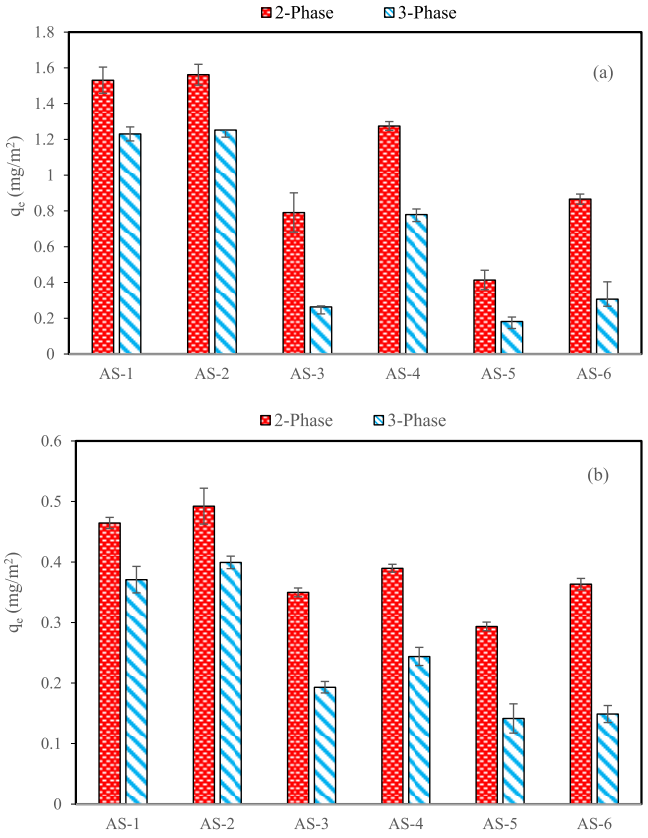

Figure 9. Influence of water on the extent of asphaltene adsorption onto (a) micro-magnetite 1 and (b) micro-magnetite 2.

particles. Due to the hydrophilic wettability of magnetite particles, these particles will be more present in the water phase and asphaltenes' adsorption is expected to be limited to the interface of water and asphaltene/toluene solution. This results in less contact of magnetite particles with asphaltene and a high reduction of asphaltene uptake. On the other hand, water is a strong displacer and deactivator fluid for the elimination of adsorbed polar hydrocarbon components on iron oxides.[61] Therefore, with the existence of water in the adsorption system, a set of factors mentioned above are involved in reducing the adsorption of asphaltenes.

3.5. Influence of Asphaltene Compositions on Asphaltene Uptake. Investigation of asphaltene adsorption on magnetite adsorbents in both static and dynamic states shows that the asphaltene uptake by magnetite adsorbents is highest in the As-2 sample, and after that, As-1, As-4, As-6, As-3, and As-5 have the highest adsorption, successively. To determine the molecular parameters governing asphaltene adsorption, the relationship between the adsorption of asphaltenes on the magnetite surface and nitrogen, sulfur, and oxygen contents of asphaltenes, asphaltenes polarity, the mean particle diameter of asphaltenes, their atomic H/C ratio, and the aromatic index obtained by FTIR analysis were investigated. It was found that the asphaltene adsorbed on the magnetite adsorbent is related to the nitrogen content of asphaltenes and their aromatic nature. As Figure 10a shows, there is a clear direct relationship between the nitrogen content of asphaltenes and their adsorption on the magnetite, such that with an increase in the nitrogen content, the adsorption extent of asphaltenes also increases. When the molecules of asphaltene are in an upward position parallel to the metal surface, bonding of N atoms with Fe can occur.[62] It is

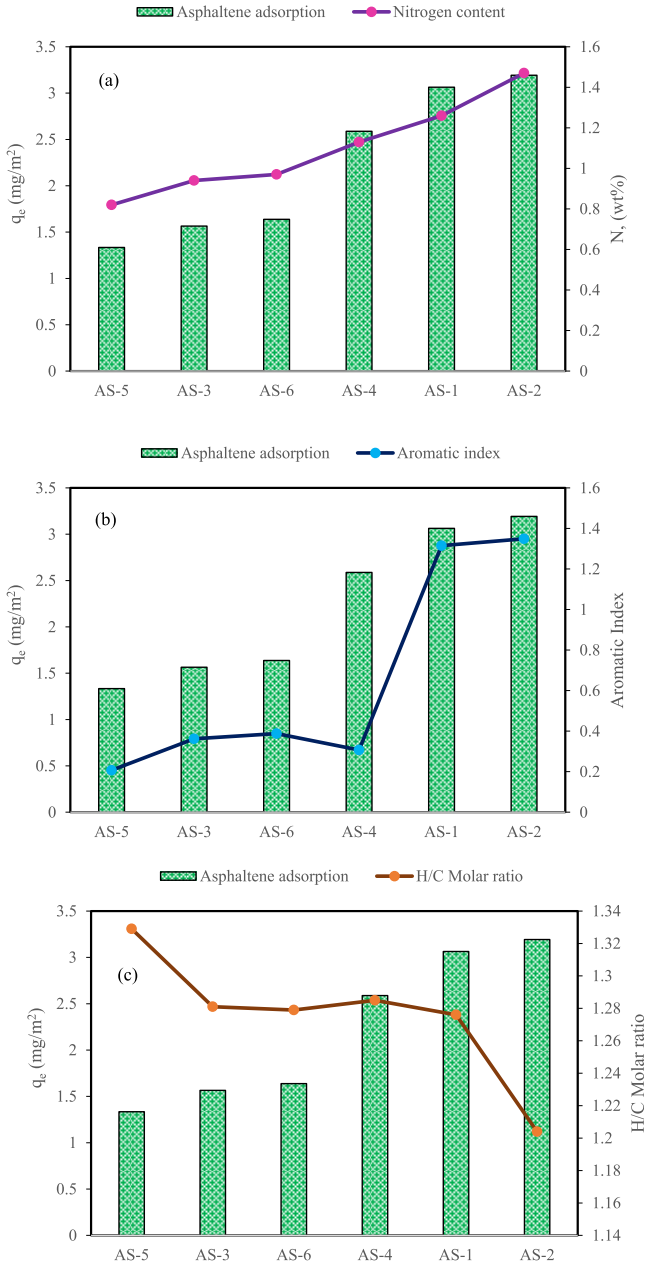

Figure 10. Correlations between asphaltene adsorption and the (a) nitrogen content, (b) aromatic index, and (c) H/C molar ratio.

noteworthy that each of the nonbasic (e.g., pyrrolic) and basic (e.g., pyridinic) nitrogen compounds are deemed as N content that can have different interactions with magnetite. However, the basic type of nitrogen has been more prone to be adsorbed onto the iron compounds than the nonbasic type.[63] On the other hand, according to Figure 10b,c, the aromatic nature of asphaltenes is also shown to be correlated with the extent of their adsorption on magnetite. The asphaltene adsorption on magnetite increased with enhancing the aromatic index obtained by FTIR analysis (Figure 10b) and declining atomic H/C ratio of asphaltenes (Figure 10c), both of which indicate the increasing effect of the aromatic nature of asphaltenes on their uptake by magnetite. Although asphaltene 4 may be slightly inconsistent with the general trend, the high uptake of this asphaltene onto the magnetite may be due to its high nitrogen content. It can be mentioned that enhancing the aromaticity of

https://doi.org/10.1021/acsomega.1c04224
ACS Omega 2021, 6, 24256−24268

Table 5. Calculated Parameters of Adsorption Isotherm Models for Asphaltene Uptake by Micro-magnetite 1

		asphaltene					
models	parameter	AS-1	AS-2[29]	AS-3	AS-4[29]	AS-5	AS-6
Langmuir	K_L (L/mg)	0.00076	0.00016	0.00056	0.00015	0.00039	0.00113
	R_L	0.5678	0.8607	0.6379	0.8668	0.7187	0.4677
	q_{max} (mg/m^2)	38.56	168.18	19.79	139.01	17.11	19.92
	R^2	0.9582	0.9985	0.9864	0.9973	0.9807	0.9895
	SD	0.1977	0.1105	0.2492	0.1266	0.2135	0.1576
Freundlich	K_F	0.0088	0.0153	0.0117	0.0094	0.0036	0.0126
	$1/n$	0.9861	0.9250	0.7421	0.9239	0.8825	0.7324
	R^2	0.9721	0.9884	0.9297	0.9831	0.9271	0.9327
	SD	0.1579	0.2114	0.2151	0.1206	0.2349	0.1982
Temkin	b_T (J/mol)	1494.88	1526.74	4721.56	1909.72	5246.17	4619.49
	K_T (L/mg)	0.0183	0.0217	0.0212	0.0188	0.0154	0.0213
	R^2	0.8904	0.9658	0.9651	0.9695	0.9201	0.9375
	SD	0.5518	0.4273	0.1103	0.4116	0.3805	0.2069
Dubinin−Radushkevich	k_{ads}	0.0008	0.0008	0.0016	0.0011	0.002	0.0014
	E (J/mol)	25	25	17.67	21.32	15.81	18.89
	q_s (mg/m^2)	7.48	8.86	3.84	7.16	2.81	3.87
	R^2	0.6688	0.7983	0.8973	0.7975	0.7691	0.8169
	SD	0.6205	0.5209	0.2984	0.5284	0.5924	0.4188

Table 6. Calculated Parameters of Adsorption Isotherm Models for Asphaltene Uptake by Micro-magnetite 2

		asphaltene					
models	parameter	AS-1	AS-2[29]	AS-3	AS-4[29]	AS-5	AS-6
Langmuir	K_L (L/mg)	0.0282	0.021	0.0204	0.0376	0.0176	0.0185
	R_L	0.0341	0.0476	0.0465	0.0258	0.0536	0.0512
	q_{max} (mg/m^2)	2.31	2.45	1.29	1.71	1.24	1.31
	R^2	0.9685	0.9601	0.9679	0.9161	0.9844	0.9735
	SD	0.2141	0.2394	0.1561	0.2921	0.2135	0.1341
Freundlich	K_F	0.3207	0.2264	0.2633	0.3232	0.2501	0.2445
	$1/n$	0.4920	0.5641	0.3692	0.4351	0.3626	0.381
	R^2	0.9998	0.9974	0.9813	0.9921	0.9888	0.9949
	SD	0.0112	0.0443	0.0799	0.0675	0.2349	0.0411
Temkin	b_T (J/mol)	1885.46	1622.15	4051.68	2431.16	4530.1	4007.79
	K_T (L/mg)	0.1703	0.1167	0.144	0.1706	0.1505	0.133
	R^2	0.9463	0.9359	0.9327	0.9018	0.9956	0.9703
	SD	0.3094	0.4083	0.1344	0.3429	0.3805	0.1017
Dubinin−Radushkevich	k_{ads}	0.00002	0.00003	0.00008	0.00002	0.0001	0.00009
	E (J/mol)	158.11	129.09	79.05	158.11	70.71	79.53
	q_s (mg/m^2)	1.81	1.83	1.08	1.52	1.02	1.09
	R^2	0.6878	0.6677	0.7348	0.6324	0.7881	0.7477
	SD	0.5331	0.5923	0.3031	0.5197	0.5923	0.3088

asphaltenes raises the molecular interaction among Fe and the π electrons of the aromatic ring.[42] Other studies have also pointed to the importance of nitrogen content and aromaticity of asphaltenes on their adsorption on solid surfaces.[64−66] Our other studies show that the mean particle diameter of asphaltenes, their polarity, and sulfur and oxygen contents of asphaltenes have no meaningful role in the adsorption of asphaltenes on magnetite, as shown in Figure S3.

3.6. Adsorption Isotherms. In this work, four isotherm models, namely, Temkin, Dubinin−Radushkevich, Freundlich, and Langmuir were utilized to model adsorption data. Standard deviation (SD) and coefficient of determination (R^2) as two statistical factors were used to measure the goodness-of-fit of adsorption data to the output of isotherm models. The mathematical formulas of these statistical factors are defined in Appendix A.

The calculated parameters of isotherm models along with SD and R^2 values achieved by fitting adsorption data to the models' response are reported in Table 5 (asphaltenes uptake by micro-magnetite 1) and Table 6 (asphaltenes uptake by micro-magnetite 2). Also, diagrams of the results of isotherm models and experimental outcomes of asphaltene adsorption on the surface of micro-magnetite adsorbents are presented in Figures S4 and S5. The adsorption of asphaltenes on the surface of micro-magnetite 1 at low concentrations is consistent with the Langmuir and Freundlich models and at higher concentrations with the Temkin model. It can be stated that due to the low specific surface area of micro-magnetite 1, adsorption occurs as a single layer and the data are consistent with the Langmuir model, and then with layer filling at higher concentrations, multilayer adsorption occurs, and adsorption data complies with the multilayer adsorption model. In the Freundlich model, values of $1/n > 1$ demonstrate weak adsorption, $0.5 < 1/n < 1$

https://doi.org/10.1021/acsomega.1c04224
ACS Omega 2021, 6, 24256−24268

indicate relatively difficult adsorption, and $0.1 < 1/n < 0.5$ show strong adsorption. The values of $1/n$ for the adsorption of asphaltenes on the surface of micro-magnetite 1 are in the range of 0.5−1, indicating that adsorption has been relatively difficult. According to the results of Table 6, the adsorption of asphaltenes on the surface of micro-magnetite 2 is well fitted to the Freundlich model, which indicates multilayer adsorption with a nonuniform distribution of uptake sites. Also, the adsorption of asphaltene 5 on the surface of micro-magnetite 2, in addition to the Freundlich model, is in good agreement with the Temkin model (Figure S5e). The values of $1/n$ in the Freundlich model for the adsorption of asphaltenes on the surface of micro-magnetite 2 are in the range of 0.1−0.5, which reveals strong adsorption. Based on the results, the specific surface area of adsorbents along with asphaltene concentration can dedicate the adsorption isotherm model.

The following equation defines an important parameter of the Langmuir isotherm, namely, dimensionless separation factor (R_L).

$$R_L = \frac{1}{1 + K_L C_0} \tag{10}$$

Basically, more desirable adsorption can be assumed with a low value of R_L. Adsorption nature is assumed to be irreversible ($R_L = 0$), unfavorable ($R_L > 1$), favorable ($0 < R_L < 1$), or linear ($R_L = 1$). The calculated R_L values reported in Tables 5 and 6 reveal that the uptake of asphaltenes on magnetite particles was appropriately favorable. However, calculated results for micro-magnetite 2 show that adsorption is more favorable having R_L values close to zero. The results of the Dubinin−Radushkevich model are important due to its parameter E presents an insight into the type of adsorption (physisorption or chemisorption). The adsorption process can happen with the mechanism of the chemical reaction (chemisorption) and particle diffusion if $E >$ 16 kJ/mol. The values of $8 < E < 16$ kJ/mol demonstrate that ion exchange is happening in the process of adsorption. Finally, the nature of adsorption is physical (physisorption) if $E < 8$ kJ/mol.[67] Although the Dubinin−Radushkevich model has the least conformity with the adsorption data in this work, E values are less than 8 kJ/mol for all cases, indicating the physisorption of asphaltenes on magnetite adsorbents.

Overall, the mechanisms of asphaltene adsorption onto magnetite were studied in this work using six asphaltene samples of various origins under static and dynamic conditions. However, investigation of surface topography before and after asphaltene uptake, the effect of higher asphaltene concentrations on adsorption isotherms, and permeability alteration due to asphaltene uptake in dynamic tests were not considered in the current work, which can also provide useful information about the adsorption of asphaltenes onto magnetite surfaces.

4. SUMMARY AND CONCLUSIONS

The main purpose of this study was to investigate the adsorption of six asphaltene samples of various origins onto the magnetite surface. The principal outcomes of this paper are summarized below:

1. The elemental analysis reveals that H/C atomic ratios of asphaltene samples are in the range of 1.2−1.3. The trend of H/C atomic ratios is consistent with the aromatic indexes obtained by FTIR analysis.
2. Based on DLS analysis, the mean particle size of asphaltenes is from 46 ± 11 to 380 ± 92 nm. A relationship was found between the sulfoxide index of FTIR analysis and the mean particle size of asphaltenes. Sulfoxide is a highly polar group, such that the higher its frequency in the sample, the lower is the solubility of asphaltene in toluene and the larger the particle size of asphaltene in the DLS analysis.
3. Enhancing the initial asphaltene concentration and the specific surface area of magnetite adsorbents (decreasing the particle size) causes an increase in the uptake of asphaltenes.
4. A significant decrease in asphaltenes uptake was observed with the addition of water to the system containing asphaltene solution and magnetite particles. The hydrophilic wettability of magnetite particles along with the competitive and blockage roles of water cause a 1.2−3 times decrease in asphaltenes uptake.
5. A decrease in asphaltene uptake was observed with an increase in the flow rate in dynamic tests, which showed that the higher flow rate reduced the interaction among the adsorbed asphaltenes and smaller asphaltene aggregates in the solution, reducing the uptake of more asphaltenes. Also, adsorbed asphaltene components with a weaker bond are detached from the magnetite surface, which can be attributed to the physisorption of asphaltenes.
6. Increase in the nitrogen content and aromatic nature of asphaltenes increases their adsorption onto the magnetite surface. The mean particle diameter of asphaltenes, their polarity, and sulfur and oxygen contents of asphaltenes have no meaningful role in the adsorption of asphaltenes on the magnetite surface.
7. The specific surface area of adsorbents along with asphaltene concentration can dedicate the adsorption isotherm model. However, the Freundlich model seems to provide better estimates for the adsorption of asphaltenes on the magnetite surface. The results of isotherm modeling show the physisorption of asphaltenes on magnetite adsorbents.

APPENDIX A: STATISTICAL FORMULAS

The following statistical factors were used to measure the goodness of fit of adsorption data to the output of isotherm models:

1. Standard Deviation (SD)

$$\mathrm{SD} = \sqrt{\frac{1}{Z-1}\sum_{i=1}^{Z}\left(\frac{q_{i,\mathrm{experimental}} - q_{i,\mathrm{predicted}}}{q_{i,\mathrm{experimental}}}\right)^2} \tag{11}$$

2. Coefficient of Determination (R_2)

$$R^2 = 1 - \frac{\sum_{i=1}^{Z}(q_{i,\mathrm{experimental}} - q_{i,\mathrm{predicted}})^2}{\sum_{i=1}^{Z}(q_{i,\mathrm{experimental}} - \overline{q_{\mathrm{experimental}}})^2} \tag{12}$$

where Z and q denote the number of data points and equilibrium adsorption (mg/m^2), respectively.

ASSOCIATED CONTENT

Supporting Information

The Supporting Information is available free of charge at https://pubs.acs.org/doi/10.1021/acsomega.1c04224.

https://doi.org/10.1021/acsomega.1c04224
ACS Omega 2021, 6, 24256−24268

Adsorption isotherm modeling and asphaltene characterizations (PDF)

AUTHOR INFORMATION

Corresponding Authors

Mohammad-Reza Mohammadi − *Department of Petroleum Engineering, Shahid Bahonar University of Kerman, Kerman 76188-68366, Iran*; Email: mohammmadi.mrm@gmail.com

Mehdi Ostadhassan − *State Key Laboratory of Continental Shale Hydrocarbon Accumulation and Efficient Development, Ministry of Education, Northeast Petroleum University, Daqing 163318, China*; Email: mehdi.ostadhassan@nepu.edu.cn

Abdolhossein Hemmati-Sarapardeh − *Department of Petroleum Engineering, Shahid Bahonar University of Kerman, Kerman 76188-68366, Iran; College of Construction Engineering, Jilin University, Changchun 130026, China*; orcid.org/0000-0002-5889-150X; Email: hemmati@uk.ac.ir, aut.hemmati@gmail.com

Authors

Sajjad Ansari − *Department of Petroleum Engineering, Shahid Bahonar University of Kerman, Kerman 76188-68366, Iran*

Hamid Bahmaninia − *Department of Petroleum Engineering, Shahid Bahonar University of Kerman, Kerman 76188-68366, Iran*

Saeid Norouzi-Apourvari − *Department of Petroleum Engineering, Shahid Bahonar University of Kerman, Kerman 76188-68366, Iran*; orcid.org/0000-0002-0410-0485

Mahin Schaffie − *Department of Petroleum Engineering, Shahid Bahonar University of Kerman, Kerman 76188-68366, Iran*

Mohammad Ranjbar − *Department of Petroleum Engineering, Shahid Bahonar University of Kerman, Kerman 76188-68366, Iran; Department of Mining Engineering, Shahid Bahonar University of Kerman, Kerman 7618868366, Iran*

Complete contact information is available at: https://pubs.acs.org/10.1021/acsomega.1c04224

Notes

The authors declare no competing financial interest.

ACKNOWLEDGMENTS

The authors thank the EOR Lab of Department of Petroleum Engineering, Shahid Bahonar University of Kerman, for providing the equipment to conduct this study.

NOMENCLATURE

XRF	X-ray fluorescence
T	temperature (K)
SD	standard deviation
R_L	separation factor
R^2	coefficient of determination
q_s	monolayer saturation capacity (mg/m^2)
Q_m	maximum adsorption amount (mg/m^2)
q_e	equilibrium adsorption (mg/m^2)
K_T	equilibrium binding constant (L/mg)
K_L	Langmuir equilibrium constant (L/mg)
K_f	Freundlich adsorption constant $\left(\frac{mg}{g}\left(\frac{L}{mg}\right)^{1/n}\right)$
k_{ads}	Dubinin−Radushkevich constant (mol^2/J^2)
ε	Polanyi potential (J^2/mol^2)
E	energy parameter of Dubinin−Radushkevich model (J/mol)
EOR	enhanced oil recovery
FTIR	Fourier transform infrared spectroscopy
DLS	dynamic light scattering
C_0	initial concentration (mg/L)
C_e	equilibrium concentration (mg/L)
b_T	Temkin constant (J/mol)
BET	Brunauer−Emmett−Teller
As	asphaltene

REFERENCES

(1) Adams, J. J. Asphaltene adsorption, a literature review. *Energy Fuels* **2014**, *28*, 2831−2856.

(2) Joonaki, E.; Burgass, R.; Hassanpouryouzband, A.; Tohidi, B. Comparison of experimental techniques for evaluation of chemistries against asphaltene aggregation and deposition: new application of high-pressure and high-temperature quartz crystal microbalance. *Energy Fuels* **2018**, *32*, 2712−2721.

(3) Piro, G.; Canonico, L. B.; Galbariggi, G.; Bertero, L.; Carniani, C. Asphaltene adsorption onto formation rock: an approach to asphaltene formation damage prevention. *SPE Prod. Facil.* **1996**, *11*, 156−160.

(4) Joonaki, E.; Hassanpouryouzband, A.; Burgass, R.; Hase, A.; Tohidi, B. Effects of Waxes and the Related Chemicals on Asphaltene Aggregation and Deposition Phenomena: Experimental and Modeling Studies. *ACS Omega* **2020**, *5*, 7124−7134.

(5) Buckley, J. S.; Liu, Y.; Xie, X.; Morrow, N. R. Asphaltenes and crude oil wetting-the effect of oil composition. *SPE J.* **1997**, *2*, 107−119.

(6) Garrouch, A. A.; Al-Ruhaimani, F. A. Simple models for permeability impairment in reservoir rocks caused by asphaltene deposition. *Pet. Sci. Technol.* **2005**, *23*, 811−826.

(7) Sim, S. S.-K.; Okatsu, K.; Takabayashi, K.; Fisher, D. B. In *Asphaltene-Induced Formation Damage: Effect of Asphaltene Particle Size and Core Permeability*, SPE Annual Technical Conference and Exhibition; Society of Petroleum Engineers, 2005.

(8) Calemma, V.; Iwanski, P.; Nali, M.; Scotti, R.; Montanari, L. Structural characterization of asphaltenes of different origins. *Energy Fuels* **1995**, *9*, 225−230.

(9) Hemmati-Sarapardeh, A.; Ameli, F.; Ahmadi, M.; Dabir, B.; Mohammadi, A. H.; Esfahanizadeh, L. Effect of asphaltene structure on its aggregation behavior in toluene-normal alkane mixtures. *J. Mol. Struct.* **2020**, No. 128605.

(10) León, O.; Rogel, E.; Espidel, J.; Torres, G. Asphaltenes: structural characterization, self-association, and stability behavior. *Energy Fuels* **2000**, *14*, 6−10.

(11) Ahooei, A.; Norouzi-Apourvari, S.; Hemmati-Sarapardeh, A.; Schaffie, M. Experimental study and modeling of asphaltene deposition on metal surfaces via electrodeposition process: The role of ultrasonic radiation, asphaltene concentration and structure. *J. Pet. Sci. Eng.* **2020**, *195*, No. 107734.

(12) Clementz, D. M. In *Alteration of Rock Properties by Adsorption of Petroleum Heavy Ends: Implications for Enhanced Oil Recovery*, SPE Enhanced Oil Recovery Symposium; Society of Petroleum Engineers, 1982.

(13) Kokal, S.; Tang, T.; Schramm, L.; Sayegh, S. Electrokinetic and adsorption properties of asphaltenes. *Colloids Surf., A* **1995**, *94*, 253−265.

(14) Wesolowski, D. J.; Machesky, M. L.; Palmer, D. A.; Anovitz, L. M. Magnetite surface charge studies to 290 C from in situ pH titrations. *Chem. Geol.* **2000**, *167*, 193−229.

(15) Tombácz, E.; Illés, E.; Majzik, A.; Hajdú, A.; Rideg, N.; Szekeres, M. Ageing in the inorganic nanoworld: example of magnetite nanoparticles in aqueous medium. *Croat. Chem. Acta* **2007**, *80*, 503−515.

(16) Jayaweera, P.; Hettiarachchi, S.; Ocken, H. Determination of the high temperature zeta potential and pH of zero charge of some transition metal oxides. *Colloids Surf., A* **1994**, *85*, 19−27.

(17) Buckley, J. Wetting alteration of solid surfaces by crude oils and their asphaltenes. *Rev. Inst. Fr. Pet.* **1998**, *53*, 303−312.
(18) Mohammed, I.; Al Shehri, D.; Mahmoud, M.; Kamal, M. S.; Alade, O. S. Impact of Iron Minerals in Promoting Wettability Alterations in Reservoir Formations. *ACS Omega* **2021**, *6*, 4022−4033.
(19) Mohammed, I.; Al Shehri, D.; Mahmoud, M.; Kamal, M. S.; Alade, O. S. A Surface Charge Approach to Investigating the Influence of Oil Contacting Clay Minerals on Wettability Alteration. *ACS Omega* **2021**, *6*, 12841−12852.
(20) Dubey, S.; Waxman, M. Asphaltene adsorption and desorption from mineral surfaces. *SPE Reservoir Eng.* **1991**, *6*, 389−395.
(21) Pernyeszi, T.; Patzkó, Á.; Berkesi, O.; Dékány, I. Asphaltene adsorption on clays and crude oil reservoir rocks. *Colloids Surf., A* **1998**, *137*, 373−384.
(22) Acevedo, S.; Ranaudo, M. A.; García, C.; Castillo, J.; Fernández, A.; Caetano, M.; Goncalvez, S. Importance of asphaltene aggregation in solution in determining the adsorption of this sample on mineral surfaces. *Colloids Surf., A* **2000**, *166*, 145−152.
(23) Marczewski, A. W.; Szymula, M. Adsorption of asphaltenes from toluene on mineral surface. *Colloids Surf., A* **2002**, *208*, 259−266.
(24) Alboudwarej, H.; Pole, D.; Svrcek, W. Y.; Yarranton, H. W. Adsorption of asphaltenes on metals. *Ind. Eng. Chem. Res.* **2005**, *44*, 5585−5592.
(25) Dudášová, D.; Flåten, G. R.; Sjöblom, J.; Øye, G. Study of asphaltenes adsorption onto different minerals and clays: Part 2. Particle characterization and suspension stability. *Colloids Surf., A* **2009**, *335*, 62−72.
(26) Syunyaev, R.; Balabin, R.; Akhatov, I.; Safieva, J. Adsorption of petroleum asphaltenes onto reservoir rock sands studied by near-infrared (NIR) spectroscopy. *Energy Fuels* **2009**, *23*, 1230−1236.
(27) Tsiamis, A.; Taylor, S. E. Adsorption behavior of asphaltenes and resins on kaolinite. *Energy Fuels* **2017**, *31*, 10576−10587.
(28) Taheri-Shakib, J.; Hosseini, S. A.; Kazemzadeh, E.; Keshavarz, V.; Rajabi-Kochi, M.; Naderi, H. Experimental and mathematical model evaluation of asphaltene fractionation based on adsorption in porous media: Dolomite reservoir rock. *Fuel* **2019**, *245*, 570−585.
(29) Mohammadi, M.-R.; Bahmaninia, H.; Ansari, S.; Hemmati-Sarapardeh, A.; Norouzi-Apourvari, S.; Schaffie, M.; Ranjbar, M. Evaluation of asphaltene adsorption on minerals of dolomite and sandstone formations in two and three-phase systems. *Adv. Geo-Energy Res.* **2021**, *5*, 39−52.
(30) González, G.; Middea, A. The properties of the calcite—solution interface in the presence of adsorbed resins or asphaltenes. *Colloids Surf.* **1988**, *33*, 217−229.
(31) Dudášová, D.; Simon, S.; Hemmingsen, P. V.; Sjöblom, J. Study of asphaltenes adsorption onto different minerals and clays: Part 1. Experimental adsorption with UV depletion detection. *Colloids Surf., A* **2008**, *317*, 1−9.
(32) Gonzalez, V.; Taylor, S. E. Asphaltene adsorption on quartz sand in the presence of pre-adsorbed water. *J. Colloid Interface Sci.* **2016**, *480*, 137−145.
(33) Khormali, A.; Sharifov, A. R.; Torba, D. I. Experimental and modeling study of asphaltene adsorption onto the reservoir rocks. *Pet. Sci. Technol.* **2018**, *36*, 1482−1489.
(34) Monjezi, R.; Ghotbi, C.; Jafari Behbahani, T.; Bakhshi, P. Experimental investigation of dynamic asphaltene adsorption on calcite packs: The impact of single and mixed-salt brine films. *Can. J. Chem. Eng.* **2019**, *97*, 2028−2038.
(35) Ezeonyeka, N. L.; Hemmati-Sarapardeh, A.; Husein, M. M. Asphaltenes adsorption onto metal oxide nanoparticles: a critical evaluation of measurement techniques. *Energy Fuels* **2018**, *32*, 2213−2223.
(36) Rezvani, H.; Kazemzadeh, Y.; Sharifi, M.; Riazi, M.; Shojaei, S. A new insight into Fe3O4-based nanocomposites for adsorption of asphaltene at the oil/water interface: an experimental interfacial study. *J. Pet. Sci. Eng.* **2019**, *177*, 786−797.
(37) Mohammadi, M.; Sedighi, M.; Hemmati-Sarapardeh, A. Application of Nanofluids in Enhanced Oil Recovery: A Systematic Literature Review and Organizing Framework. In *Nanofluids and Their Engineering Applications*; CRC Press, 2019; pp 433−451.
(38) Mazloom, M. S.; Hemmati-Sarapardeh, A.; Husein, M. M.; Behbahani, H. S.; Zendehboudi, S. Application of nanoparticles for asphaltenes adsorption and oxidation: A critical review of challenges and recent progress. *Fuel* **2020**, *279*, No. 117763.
(39) Ali, A. M.; Yahya, N.; Qureshi, S. Interactions of ferro-nanoparticles (hematite and magnetite) with reservoir sandstone: implications for surface adsorption and interfacial tension reduction. *Pet. Sci.* **2020**, 1037−1055.
(40) Tazikeh, S.; Amin, J. S.; Zendehboudi, S.; Dejam, M.; Chatzis, I. Bi-fractal and bi-Gaussian theories to evaluate impact of polythiophene-coated Fe3O4 nanoparticles on asphaltene precipitation and surface topography. *Fuel* **2020**, *272*, No. 117535.
(41) Kazemzadeh, Y.; Eshraghi, S. E.; Kazemi, K.; Sourani, S.; Mehrabi, M.; Ahmadi, Y. Behavior of asphaltene adsorption onto the metal oxide nanoparticle surface and its effect on heavy oil recovery. *Ind. Eng. Chem. Res.* **2015**, *54*, 233−239.
(42) Nassar, N. N.; Hassan, A.; Carbognani, L.; Lopez-Linares, F.; Pereira-Almao, P. Iron oxide nanoparticles for rapid adsorption and enhanced catalytic oxidation of thermally cracked asphaltenes. *Fuel* **2012**, *95*, 257−262.
(43) Tazikeh, S.; Kondori, J.; Zendehboudi, S.; Amin, J. S.; Khan, F. Molecular dynamics simulation to investigate the effect of poly-thiophene-coated Fe3O4 nanoparticles on asphaltene precipitation. *Chem. Eng. Sci.* **2021**, *237*, No. 116417.
(44) Mousavi, S.-P.; Hemmati-Sarapardeh, A.; Norouzi-Apourvari, S.; Jalalvand, M.; Schaffie, M.; Ranjbar, M. Toward mechanistic understanding of wettability alteration in calcite and dolomite rocks: The effects of resin, asphaltene, anionic surfactant, and hydrophilic nano particles. *J. Mol. Liq.* **2021**, *321*, No. 114672.
(45) Bahmaninia, H.; Ansari, S.; Mohammadi, M.-R.; Norouzi-Apourvari, S.; Hemmati-Sarapardeh, A.; Schaffie, M.; Ranjbar, M. Toward mechanistic understanding of asphaltene adsorption onto quartz surface: The roles of size, concentration, and hydrophobicity of quartz, asphaltene composition, flow condition, and aqueous phase. *J. Pet. Sci. Eng.* **2021**, No. 108820.
(46) Zdravkov, B.; Čermák, J.; Šefara, M.; Janku, J. Pore classification in the characterization of porous materials: A perspective. *Open Chem.* **2007**, *5*, 385−395.
(47) Dastgerdi, Z. H.; Meshkat, S. S.; Hosseinzadeh, S.; Esrafili, M. D. Application of novel Fe 3 O 4−polyaniline nanocomposites in asphaltene adsorptive removal: equilibrium, kinetic study and DFT calculations. *J. Inorg. Organomet. Polym. Mater.* **2019**, *29*, 1160−1170.
(48) Shayan, N. N.; Mirzayi, B. Adsorption and removal of asphaltene using synthesized maghemite and hematite nanoparticles. *Energy Fuels* **2015**, *29*, 1397−1406.
(49) Dehaghani, A. H. S.; Daneshfar, R. How much would silica nanoparticles enhance the performance of low-salinity water flooding? *Pet. Sci.* **2019**, *16*, 591−605.
(50) Wang, J.; Buckley, J.PRRC, New Mexico Tech. *Standard Procedure for Separating Asphaltenes from Crude Oils*; Petroleum Recovery Research Center, 2002.
(51) Kecili, R.; Hussain, C. M. Mechanism of Adsorption on Nanomaterials. In *Nanomaterials in Chromatography*; Elsevier, 2018; pp 89−115.
(52) Foo, K. Y.; Hameed, B. H. Insights into the modeling of adsorption isotherm systems. *Chem. Eng. J.* **2010**, *156*, 2−10.
(53) Langmuir, I. The constitution and fundamental properties of solids and liquids. Part I. Solids. *J. Am. Chem. Soc.* **1916**, *38*, 2221−2295.
(54) Zhao, B.; Shaw, J. M. Composition and size distribution of coherent nanostructures in Athabasca bitumen and Maya crude oil. *Energy Fuels* **2007**, *21*, 2795−2804.
(55) Asemani, M.; Rabbani, A. R. Detailed FTIR spectroscopy characterization of crude oil extracted asphaltenes: Curve resolve of overlapping bands. *J. Pet. Sci. Eng.* **2020**, *185*, No. 106618.
(56) Hemmati-Sarapardeh, A.; Dabir, B.; Ahmadi, M.; Mohammadi, A. H.; Husein, M. M. Toward mechanistic understanding of asphaltene aggregation behavior in toluene: the roles of asphaltene structure, aging

https://doi.org/10.1021/acsomega.1c04224
ACS Omega 2021, 6, 24256−24268

time, temperature, and ultrasonic radiation. *J. Mol. Liq.* **2018**, *264*, 410−424.
(57) Asemani, M.; Rabbani, A. R. Oil-oil correlation by FTIR spectroscopy of asphaltene samples. *Geosci. J.* **2016**, *20*, 273−283.
(58) Lamontagne, J.; Dumas, P.; Mouillet, V.; Kister, J. Comparison by Fourier transform infrared (FTIR) spectroscopy of different ageing techniques: application to road bitumens. *Fuel* **2001**, *80*, 483−488.
(59) Groenzin, H.; Mullins, O. C. Molecular size and structure of asphaltenes from various sources. *Energy Fuels* **2000**, *14*, 677−684.
(60) Hassanpouryouzband, A.; Joonaki, E.; Taghikhani, V.; Bozorgmehry Boozarjomehry, R.; Chapoy, A.; Tohidi, B. New two-dimensional particle-scale model to simulate asphaltene deposition in wellbores and pipelines. *Energy Fuels* **2018**, *32*, 2661−2672.
(61) Carbognani, L. Effects of iron compounds on the retention of oil polar hydrocarbons over solid sorbents. *Pet. Sci. Technol.* **2000**, *18*, 335−360.
(62) Ortega-Rodriguez, A.; Alvarez-Ramirez, F.; Cruz, S.; Lira-Galeana, C. A model to calculate the average interaction energy and adhesion force between petroleum asphaltenes and some metallic surfaces. *J. Colloid Interface Sci.* **2006**, *301*, 352−359.
(63) Habeeb, J. J. Method for selectively removing basic nitrogen compounds from lube oils using transition metal halides or transition metal tetrafluoroborates. U.S. Patent No. 4,329,222, 1982. U.S. Patent and Trademark Office: Washington, DC. https://patents.google.com/patent/US4329222A/en.
(64) López-Linares, F.; Carbognani, L.; Sosa-Stull, C.; Pereira-Almao, P.; Spencer, R. J. Adsorption of virgin and visbroken residue asphaltenes over solid surfaces. 1. Kaolin, smectite clay minerals, and athabasca siltstone. *Energy Fuels* **2009**, *23*, 1901−1908.
(65) Lopez-Linares, F.; Carbognani, L.; Hassan, A.; Pereira-Almao, P.; Rogel, E.; Ovalles, C.; Pradhan, A.; Zintsmaster, J. Adsorption of Athabasca vacuum residues and their visbroken products over macroporous solids: influence of their molecular characteristics. *Energy Fuels* **2011**, *25*, 4049−4054.
(66) López-Linares, F.; Carbognani, L.; Spencer, R. J.; Pereira-Almao, P. Adsorption studies in Athabasca core sample: Virgin and mild thermal cracked residua. *Energy Fuels* **2011**, *25*, 3657−3662.
(67) Inam, E.; Etim, U.; Akpabio, E.; Umoren, S. Process optimization for the application of carbon from plantain peels in dye abstraction. *J. Taibah Univ. Sci.* **2017**, *11*, 173−185.

https://doi.org/10.1021/acsomega.1c04224
ACS Omega 2021, 6, 24256−24268